

MEASUREMENT OF THE TENSILE STRESSES  
BEHIND A SPALLING PLANE

V. D. Gluzman and G. I. Kanel'

UDC 532.593

When a compression pulse is reflected from the free surface of a specimen, tensile stresses are produced that may lead to failure: spalling [1]. Measurements on spalling strength are indirect, so the published data may differ by an order of magnitude even for similar loading conditions [2]. Recording the speed of the free surface gives the most reliable information on the tensile stresses in the spalling plane and in other sections of the spalling material, but it does not give information on the subsequent growth of the process as the reflected negative-pressure wave propagates from the spalling plane into the specimen. A study of the phenomenon within the framework of the continual kinetic failure model [3] shows that the stress relaxation during failure restricts the growth of the tensile-stress amplitudes in the reflected wave. Here we propose a method of measuring the tensile-stress amplitudes behind the cleavage plane for M2 copper and Kh18N10T stainless steel.

It is impossible to measure directly the tensile stresses occurring under conditions of one-dimensional dynamic deformation. However, when a compression or tension wave is reflected from a contact boundary with a material having lower dynamic rigidity, the sign of the loading reverses [1]. One can select a pair of materials differing in compressibility in such a way that a compressive shock wave on conversion to a reflected wave at a boundary between hard and soft materials leaves the pressure at the contact boundary positive, even if it attains large negative values in the hard material, and it can then be recorded for example with manganin transducers. The tensile-stress amplitudes in the hard specimen near the boundary can then be derived by examining the wave interactions on the basis of the  $p(t)$  pressure profile recording at the boundary.

Two series of experiments with stainless steel and copper were performed to examine these stresses. In the first series, capacitative transducers were used [4] to record  $w(t)$ , the velocity profile for the free surface. Figure 1 shows the results, where curves 1 and 2 were obtained with specimens of Kh18N10T steel of thicknesses 15 and 10 mm correspondingly, while curves 3 and 4 were recorded with copper specimens of thickness 12 mm. The compression wave of short duration was produced by collision of an aluminum plate of thickness 2 mm accelerated to a speed of  $450 \pm 20$  m/sec, while a wave of large duration was generated by a plane-wave generator (explosive lens) in contact with the specimen. The compression-corresponding amplitude could be varied in the latter case.

The tensile stresses in the spalling plane were determined to a first approximation from the difference  $\Delta w$  at the first maximum in  $w(t)$  and the first minimum [5]:

$$\sigma^* = (1/2)\rho_0 c_0 \Delta w,$$

where  $\rho_0$  is the density of the material and  $c_0$  is the bulk speed of sound. Stainless steel has a pronounced elastic precursor on  $w(t)$ ; a correction  $\delta w$  [6] was introduced for this material to allow for the leading part of the spalling pulse, which propagates with the speed  $c_l$  of a longitudinal elastic wave, together with the unloading part of the incident compression pulse, which has a speed of about  $c_0$ :

$$\sigma^{**} = (1/2)\rho_0 c_0 (\Delta w + \delta w),$$

where  $\delta w$  was determined in the following form on the basis of the velocity gradients in the incident negative-pressure wave  $\dot{w}_1$  and in the spalling-pulse front  $\dot{w}_2$ :

$$\delta w = \left( \frac{h}{c_0} - \frac{h}{c_l} \right) \frac{\dot{w}_1 \dot{w}_2}{\dot{w}_1 + \dot{w}_2},$$

Chernogolovka. Translated from Zhurnal Prikladnoi Mekhaniki i Tekhnicheskoi Fiziki, No. 4, pp. 146-150, July-August, 1983. Original article submitted June 15, 1982.

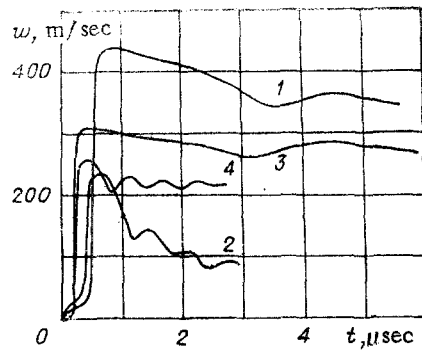


Fig. 1

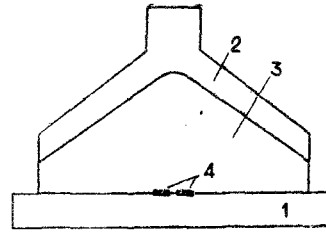


Fig. 2

Here  $h$  is the thickness of the spalled plate, as determined from the reverberation period of the spalling pulse. Table 1 summarizes the results. The values obtained for the spalling strength of copper agree satisfactorily with those of [6].

The experiments on the tensile stresses behind the spalling plane were performed with the apparatus shown in Fig. 2. The shock-wave loading of the specimen 1 was provided by exploding a plane-wave generator of diameter 100 mm consisting of the conical explosive layer 2 and the wax insert 3. At the boundary between the wax and the specimen there were manganin pressure transducers 4, which were separated from the specimen and the wax by PTFE inserts of 0.2 mm on each side. The loading conditions were identical with those used in recording profiles 1 and 3 in Fig. 1. The thickness of the specimens was 12 mm. Figure 3a and b show the waveforms with copper and stainless steel. These record the arrival of the shock wave at the contact boundary, the fall in pressure arising from the tension wave following the shock wave, and the additional fall in pressure 1-2 with the arrival at the contact boundary of the tension wave reflected from the free surface. The pressures in the shock wave and at the points 1 and 2 were determined directly from the waveforms. Allowance was made for the hysteresis in the readings of the manganin transducers [7]. On the basis of [7, 8], the relationship between the pressure  $p$  and the relative change in resistance  $\Delta R/R_0$  for the shock waves of amplitude 7-20 GPa was put in the form

$$p = (\Delta R/R_0 - 0.0237)39.04 \text{ GPa.}$$

To improve the accuracy, most of the experiments were performed with excess amplification (Fig. 3b and d), so that the reflected tension wave was represented on the working part of the screen with the best resolution. The method of determining the pressure in the tail of the tension wave corresponding to point 2 on  $p(t)$  is indicated by the diagrams of time  $t$  against coordinate  $x$  and of pressure  $p$  against mass velocity  $u$  in Fig. 4. Points 1 and 2 in Fig. 4 correspond to those indicated on the waveform. The line O12 in the  $t-x$  diagram shows the path of the contact boundary and the disposition of the pressure transducer. At point O, a shock wave of amplitude  $p_0$  is injected into the specimen, whose path is shown by the line OA. At moderate shock-compression pressures the isentrope for unloading of the metal is represented closely in  $p-u$  coordinates by the shock-wave adiabatic [1]. In that case, a one-dimensional compression pulse is a simple wave, and the change in state at the contact boundary up to arrival of the reflected tension wave is described in  $p-u$  coordinates by curve O1, which coincides with the shock adiabatic. After the emergence of the shock wave at the free surface, a reflected tension wave arises, which is described by lines A1 and A2 in the  $t-x$  diagram. Starting at instant  $t_1$  (the arrival of the reflected tension-wave front at the boundary), the change in state on the  $p-u$  diagram at the boundary deviates from curve O1 and is determined by the intersection of the paths representing the state change along the corresponding  $C_+$  characteristic for the incident tension wave in the wax and the  $C_-$  characteristic for the reflected tension wave in the specimen. For example, the state at point 2 is determined by the intersection of the wax isentrope 2'2 and the copper isentrope K2. The pressure at the point in the specimen K near the contact surface corresponds to intersection of the paths for the state change along the  $C_+$  characteristic 1K in the specimen and the  $C_-$  characteristic K2. The position of the 1K isentrope in the  $p-u$  diagram is determined from the measured pressure  $p_1$ . Experiment also gives the pressure at point 2, from which one can find the position of the isentrope K2 if one knows the path followed by the state change 2'2 for the wax along the  $C_+$  characteristic B2. The position of

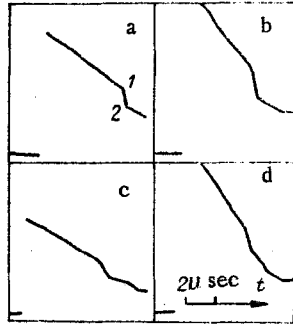


Fig. 3

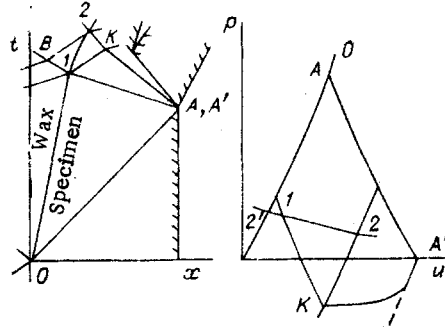


Fig. 4

the latter is determined from the pressure at point 2', which is determined from the experimental p-t recordings by extrapolating the initial part to time t<sub>2</sub>.

Allowance for the elastoplastic properties of the material causes these paths to shift in the p-u diagram, but because all states of the material correspond to the region of plastic strain, that allowance has very little effect on the accuracy in determining the pressure at point K.

Table 2 gives the pressures at points 0, 1, 2, and 2' obtained from sets of four measurements and the amplitudes of the tensile stresses p<sub>K</sub> calculated from these data. The calculations were based on the shock adiabat for copper in the form D = 3.95 + 1.45u (km/sec) and that for wax as D = 2.96 + 1.53u (km/sec) [9]. A minor correction was made in determining p<sub>2</sub>', which allows for the reduction in the speed of sound along the B2 characteristic as the pressure falls.

The value of p<sub>K</sub> determined in this way is subject to various sources of error such as possible deviations from one-dimensional, discrepancy between the shock adiabatics and the unloading isentropes for the materials, and the deviations in the hysteresis in the manganin transducers from the average value δR/R<sub>0</sub> = 0.0237. To estimate the overall error of measurement we performed additional experiments with previously slit specimens of copper and stainless steel. In these experiments, a specimen of overall thickness 12 mm was made up of two plates, and since negative pressure is impossible in the plane of section, the pressure at point K can be estimated from the recorded pressure profile on part 01. In particular, if there is no failure in the thin plate facing the wax, then the pressure at point K is given by

$$p'_K = \dot{p}_{av} [2h/c_0 - (t_2 - t_1)].$$

Figure 3c and d show waveforms obtained with compound copper and steel specimens correspondingly, while the results are given in Table 2. Comparison of p<sub>K</sub> and p<sub>K</sub>' shows that the amplitudes found for the tensile stresses may be too low by 0.3-0.4 GPa for copper and 0.4-0.6 GPa for steel. Therefore, at a distance of 4-5 mm behind the spalling plane the amplitudes of the tensile stresses are 1.2-1.6 GPa for copper and 1.5-2.1 GPa for stainless steel. These values may be compared with the spalling strengths found from the w(t) profiles, and it is clear that copper may show some increase in the maximal tensile stresses as the reflected tension wave propagates from the spalling plane, while in stainless steel the maximal tensile stresses are virtually restricted to the spalling strength. This conclusion for the

TABLE 1

Material	Thickness, mm	Loading conditions	$\Delta w$ , m/sec	$h$ , mm	$\dot{v}_1$ , 10 <sup>6</sup> m/sec <sup>2</sup>	$\dot{v}_2$ , 10 <sup>6</sup> m/sec <sup>2</sup>	$\sigma^*$ , GPa	$\sigma^{**}$ , GPa
M2 Copper	12	Explosive lens	45±6	6	22	30	0.8±0,1	--
»	12	Striker	62±4	1,1	290	165	1,1±0,1	
Kh18N10T stainless steel	45	Explosive lens	95±6	6,9	50±5	27±3	1,7±0,1	1,8±0,1
	10	Striker	106±7	1,8	350±35	90±10	1,9±0,1	2,0±0,1

TABLE 2

Material	Thickness, mm	$p_0$ , GPa	$p_1$ , GPa	$p_2$ , GPa	$\beta_0$ , GPa	$\nu_K$ , GPa	$\nu'_K$ , GPa
M2 copper	12	7.04	3.36	2.04	3.1	$-1.22 \pm 0.15$	--
»	4+8	7.04	3.36	2.17	3.1	$-0.66 \pm 0.15$	$-1.0 \pm 0.15$
Kh18N10T	12	10.1	4.46	2.53	3.98	$-1.55 \pm 0.3$	--
	6+6	10.1	4.46	2.54	3.98	$-1.51 \pm 0.1$	--
	3+9	10.1	4.46	2.79	3.98	$-0.49 \pm 0.2$	$-1.0 \pm 0.1$

stainless steel is confirmed by the data of Table 2 for solid specimens and for specimens made up of 6-mm plates. The differences in the variation in tensile stress behind the spalling plane correlate with the values given in Table 1 for the strength realized in spalling as a function of the characteristic duration of the initial load.

These tensile-stress measurements behind the spalling plane can be used to construct kinetic failure models. The experiments with stainless steel show in particular that the initial rate of the process is fairly large in spite of the duration of the final failure stage.

We are indebted to V. E. Fortov for discussion and to G. A. Savel'eva for assistance in preparing and performing the measurements.

## LITERATURE CITED

1. Ya. B. Zel'dovich and Yu. P. Raizer, *Physics of Shock Waves and High-Temperature Hydrodynamic Phenomena* [in Russian], Nauka, Moscow (1966).
2. G. I. Kanel', "The resistance of a metal to spalling failure," *Fiz. Goreniya Vzryva*, No. 3 (1982).
3. G. I. Kanel' and L. G. Chernykh, "The spalling failure process," *Zh. Prikl. Mekh. Tekh. Fiz.*, No. 6 (1980).
4. A. G. Ivanov and S. A. Novikov, "The capacitance-transducer method for recording the instantaneous velocity of a moving surface," *Prib. Tekh. Eksp.*, No. 1 (1963).
5. S. A. Novikov, I. I. Divnov, and A. G. Ivanov, "A study of the failure in steel, aluminum, and copper on explosive loading," *Fiz. Met. Metalloved.*, 25, No. 4 (1964).
6. V. I. Romanchenko and G. V. Stepanov, "Dependence of the critical stresses on the loading-time parameters in spalling for copper, aluminum, and steel," *Zh. Prikl. Mekh. Tekh. Fiz.*, No. 4 (1980).
7. G. I. Kanel', G. G. Vakhitova, and A. N. Dremín, "Metrological characteristics of manganese pressure transducers under conditions of shock compression and unloading," *Fiz. Goreniya Vzryva*, No. 2 (1978).
8. A. V. Anan'in, A. N. Dremín, and G. I. Kanel', "Polymorphic transformation of iron in a shock wave," *Fiz. Goreniya Vzryva*, No. 3 (1981).
9. R. McCouin, S. Marsh, et al., "Equations of state for solids indicated by shock-wave studies," in: *High-Velocity Shock Phenomena* [Russian translation], Mir, Moscow (1973).